An open system approach towards the simulation of chemomechanically induced concrete failure

Ellen Kuhl, Andreas Menzel & Paul Steinmann
Chair of Applied Mechanics
Technical University of Kaiserslautern, PO Box 3049
D-67653 Kaiserslautern, Germany
e-mail: ekuhl@rhrk.uni-kl.de, amenzel@rhrk.uni-kl.de, ps@rhrk.uni-kl.de

ABSTRACT: The present contribution aims at deriving a chemomechanical damage model within the framework of open system thermodynamics. The governing equations, which are essentially characterized through the balance of mass and momentum of the chemical reactant, are discretized with the help of the finite element method. The central idea is the reformulation of the classical damage variable in terms of the non–constant reference density, which is then introduced as nodal degree of freedom next to the deformation itself. The basic features of the derived model will be discussed with the help of selected computational examples.

Keywords: open system thermodynamics, time dependent damage, concrete failure, absolut chemomechanics.

1 INTRODUCTION

It is well–known, that concrete structures subjected to changing water level or constant water flow exhibit not only mechanically induced damage. Rather, their stiffness is reduced significantly as they undergo permanent chemical reactions with the surrounding ground water. Due to the chemically induced dissolution of the cementitious skeleton, a remarkable increase of porosity can be observed which, in turn, accelerates the accumulation of mechanical damage related to stiffness degradation. On the other hand, the increase of porosity, or rather decrease in density, manifests itself in a local increase of permeability which accelerates further dissolution due to improved transport properties for the solved ions. Chemical and mechanical effects are thus interacting in a complex manner and typically result in a considerable reduction of life time. The above phenomenon is particularly relevant in the context of long-time durability prediction, e.g. for containers of radioactive waste, see e.g. (Coussy 1995), (Torrenti, Mainguy, Adenot, and Tognazzi 1998), (Carmeliet 1998), (Ulm and Coussy 1995; Ulm, Torrenti, and Adenot 1999), (Kuhl and Meschke 2002; Kuhl 2003).

The present contribution is concerned with the derivation of a theoretical and computational model for chemomechanically coupled problems. To this end, we will make use of the framework of open system thermodynamics, whereby the chemical reactant, in this context the cementitious skeleton, is considered as an open system which is allowed to constantly gain or lose mass. In the case of chemically reacting concrete, dissolution of portlandite or ettringite and the progressive decalcification of the calcium silicate hydrates represent typical examples of mass sources while the transport of the solved cations and anions manifests itself in an additional mass flux. Consequently, the classical conservation law of mass has to be recast into a balance equation balancing the rate of change of the mass of the reactant with a possible mass source or rather sink term, and an in- or rather outflux of matter. This enhanced mass balance typically has a direct impact on the balance equations of momentum, kinetic energy, energy and entropy of the open system. In contrast to the theory of porous media documented by (Truesdell and Toupin 1960), (Bowen 1976), (Coussy 1995), (de Boer 2000), the theory of open systems is based on the fundamental assumption that the constituents, in this context the cementitious skeleton and the reacting fluid, are not superposed locally but are rather spatially separated. Moreover, the overall behavior is assumed to be determined primarily by the response of the cement matrix which is allowed to undergo a permanent exchange of mass, momentum, energy and entropy with its environment, compare also (Katchalsky and Curran 1965), (Epstein

1

and Maugin 2000), (Kuhl and Steinmann 2003d; Kuhl and Steinmann 2003b).

The chemomechanical problem is thus primarily governed by the balance of mass and momentum of the cementitious skeleton. It turns out, that the former can alternatively be interpreted as the damage evolution law, whereby the damage variable d is directly related to the material density ρ_0 as $d = 1 - \rho_0/\rho_0^*$ with ρ_0^* denoting the reference density of the intact material. The damage variable thus gains a real physical interpretation and can be measured experimentally just by measuring the current density. The temporal discretization of the governing equations is carried out with the implicit Euler backward scheme while for the spatial discretization, we suggest a monolithic two–field finite element formulation by introducing both, the local density and the deformation as primary unknowns on the nodal level. The nonlinear set of discrete equations is solved with the help of the incremental iterative Newton-Raphson scheme supplemented by a consistent linearization as described in detail in (Kuhl and Steinmann 2003e; Kuhl and Steinmann 2003c; Kuhl and Steinmann 2003a).

This contribution is organized as follows. After introducing the basic kinematics, the balance equations, the constitutive equations and the corresponding weak form of open system thermodynamics in section 2, we will derive the temporal and spatial discretization in section 3 followed by its consistent linearization in section 4. Finally selected examples will be discussed in section 5.

2 CONTINUOUS EQUATIONS

2.1 *Kinematics*

Let $\mathcal{B}_0$ and $\mathcal{B}_t$ denote the reference and current configuration occupied by the body of interest at time t_0 and $t \in \mathbb{R}$, respectively. Then the kinematic description is basically characterized through the deformation map $\boldsymbol{\varphi}$ mapping the material placement $\boldsymbol{X}$ in the material configuration $\mathcal{B}_0$ to its spatial placement $\boldsymbol{x}$ in the spatial configuration $\mathcal{B}_t$.

$$\boldsymbol{x} = \boldsymbol{\varphi}\,(\,\boldsymbol{X},t\,): \quad \mathcal{B}_0 \times \mathbb{R} \to \mathcal{B}_t \qquad (1)$$

The corresponding deformation gradient $\boldsymbol{F}$ characterizes the linear tangent map from the material tangent space $T\mathcal{B}_0$ to the spatial tangent space $T\mathcal{B}_t$.

$$\boldsymbol{F} = \nabla \boldsymbol{\varphi}\,(\,\boldsymbol{X},t\,): \quad T\mathcal{B}_0 \to T\mathcal{B}_t \qquad (2)$$

Its determinant defines the related Jacobian J as $J = \det \boldsymbol{F} > 0$. In what follows, $\mathrm{D}_t = \partial_t \{\bullet\}|_X$ will denote the material time derivative of a quantity $\{\bullet\}$ at fixed material placement $\boldsymbol{X}$. Accordingly, the spatial velocity $\boldsymbol{v} = \mathrm{D}_t \boldsymbol{\varphi}\,(\,\boldsymbol{X},t\,)$ can be understood as the material time derivative of the deformation map $\boldsymbol{\varphi}$. We shall apply a formulation which is entirely related to

the material frame of reference $\mathcal{B}_0$. Thus, $\nabla\{\bullet\}$ and $\mathrm{Div}\,\{\bullet\}$ denote the gradient and the divergence of any field $\{\bullet\}$ with respect to the material placement $\boldsymbol{X}$.

2.2 *Balance equations*

The present section briefly summarizes the relevant balance equations for open system thermodynamics which constitute the basis for the finite element analysis to be derived later on. Unlike classical closed systems typically found in traditional mechanical applications, open systems exhibit a permanent exchange of mass, momentum, energy and entropy with their environment, compare (Kuhl and Steinmann 2003d; Kuhl and Steinmann 2003b; Kuhl and Steinmann 2003e). As a natural consequence, the classical balance of mass $\mathrm{D}_t\,\rho_0 = 0$ has to be enhanced by an additional mass flux $\boldsymbol{R}$ and a mass source $\mathcal{R}_0$.

$$\mathrm{D}_t\,\rho_0 = \mathrm{Div}\,\boldsymbol{R} + \mathcal{R}_0 \qquad (3)$$

The mass specific balance of momentum

$$\rho_0\,\mathrm{D}_t\,\boldsymbol{p} = \mathrm{Div}\,\bar{\boldsymbol{\Pi}}^t + \bar{\boldsymbol{b}}_0 \qquad (4)$$

balances the rate of change of the mass specific momentum density $\boldsymbol{p} = \boldsymbol{v}$ with the reduced momentum flux $\bar{\boldsymbol{\Pi}}^t$ and the reduced momentum source $\bar{\boldsymbol{b}}_0$. The Clausius–Duhem inequality for open system thermodynamics can then be expressed in the following form,

$$\bar{\mathrm{d}}_0 = \bar{\boldsymbol{\Pi}}^t : \mathrm{D}_t \boldsymbol{F} - \rho_0 \mathrm{D}_t \psi + \theta\,[\,\mathrm{Div}\,\boldsymbol{S} - \mathcal{S}_0\,] \geq 0 \quad (5)$$

whereby the non–standard extra terms $\boldsymbol{S}$ and $\mathcal{S}_0$ have been included accounting for the explicit exchange of entropy with the outside world. By introducing a free Helmholtz energy of the following form $\psi = \psi\,(\,\rho_0, \boldsymbol{F}\,)$ we straightforwardly obtain the definition of the reduced first Piola–Kirchhoff stress $\bar{\boldsymbol{\Pi}}^t$

$$\bar{\boldsymbol{\Pi}}^t = \rho_0\,\mathrm{D}_{\boldsymbol{F}}\psi \qquad (6)$$

as thermodynamically conjugate variables to the spatial motion deformation gradient $\boldsymbol{F}$. Moreover, we are left with the additional restrictions

$$\bar{\mathrm{d}}_0 - \rho_0\,\mathrm{D}_{\rho_0}[\,\mathrm{Div}\,\boldsymbol{R} - \mathcal{R}_0\,] + \theta\,\mathrm{Div}\,\boldsymbol{S} - \mathcal{S}_0\,] \geq 0 \quad (7)$$

for the constitutive assumptions for the extra external entropy flux $\boldsymbol{S}$ and the extra external entropy source $\mathcal{S}_0$ which ensure that the overall dissipation does not become negative.

Remark 2.1: Interpretation of the balance of mass
Within the framework of chemomechanics, in particular in the context of leaching, the balance of mass (3) typically expresses the evolution of the moisture content in terms of the moisture flux.

2.3 Constitutive equations

To close the set of governing equations, we shall introduce constitutive assumptions for the reduced momentum flux $\bar{\boldsymbol{\Pi}}^t$, the reduced momentum source $\bar{\boldsymbol{b}}$, the mass flux $\boldsymbol{R}$, the mass source $\mathcal{R}_0$, the extra entropy flux $\boldsymbol{S}$ and the extra entropy source $\mathcal{S}_0$. For the particular case of chemomechanical damage to be considered in the sequel, the chemical reactant can be considered as an open system which is allowed to constantly gain or lose mass due to moisture transport in combination with chemical reactions. The fundamental idea is to introduce a damage variable d as

$$d = 1 - \rho_0 / \rho_0^* \qquad (8)$$

which can thus be interpreted as the change in the density ρ_0 with respect to a reference density ρ_0^*. The Helmholtz free energy density ψ can then be expressed in the following familiar format,

$$\psi = [1 - d]\,\psi^{\text{neo}} \qquad (9)$$

in terms of the current amount of damage $[1 - d]$ and the classical Neo–Hookean free energy ψ^{neo}.

$$\psi^{\text{neo}} = \frac{1}{\rho_0}\Big[\frac{1}{2}\lambda_0 \ln^2(J) + \frac{1}{2}\mu_0[\boldsymbol{F} : \boldsymbol{F} - n^{\text{dim}} - 2\ln(J)]\Big] \qquad (10)$$

The momentum flux $\bar{\boldsymbol{\Pi}}^t$ or rather the reduced first Piola–Kirchhoff stress tensor follows straightforwardly from the evaluation of the dissipation inequality (6) as $\bar{\boldsymbol{\Pi}}^t = \rho_0\, \mathrm{D}_{\boldsymbol{F}}\psi$.

$$\bar{\boldsymbol{\Pi}}^t = [1 - d]\,\bar{\boldsymbol{\Pi}}^{\text{neo}t} \qquad (11)$$

It can thus be expressed as the classical Neo–Hookean stress tensor $\boldsymbol{\Pi}^{\text{neo}t}$

$$\bar{\boldsymbol{\Pi}}^{\text{neo}t} = [\lambda_0 \ln(J) - \mu_0]\,\boldsymbol{F}^{-t} + \mu_0\,\boldsymbol{F} \qquad (12)$$

weighted by the current amount of damage $[1 - d]$. For the sake of simplicity, we shall assume that the reduced momentum source, i.e. the volume force vector $\bar{\boldsymbol{b}}_0$ vanishes identically.

$$\bar{\boldsymbol{b}}_0 = \boldsymbol{0} \qquad (13)$$

In analogy to Fick's law, the mass flux $\boldsymbol{R}$ is related to the gradient of the density $\nabla\rho_0$

$$\boldsymbol{R} = R_0\,\nabla\rho_0 \qquad (14)$$

which can be related to the gradient of the damage variable d as $\nabla\rho_0 = -\rho_0^*\,\nabla d$. Herein, R_0 denotes the materially isotropic mass conduction coefficient. Note, that in the case of progressive damage, it might seem reasonable to related the mass conduction coefficient to the reduced cross section area as

$\boldsymbol{R} = R_0\,/\,[1 - d]\,\nabla\rho_0$. Finally, we introduce a mass source $\mathcal{R}_0$ of the following format.

$$\mathcal{R}_0 = -\rho_0^*\exp\Big[-\alpha\,\frac{1}{1-d}\frac{\psi_0^*}{\psi_0^{\text{neo}}}\Big] \qquad (15)$$

Alternatively, by making use of equation (9) as $\psi_0 = [1 - d]\,\psi_0^{\text{neo}}$, the above equation can be expressed as follows $\mathcal{R}_0 = -\rho_0^*\exp[-\alpha\,\psi_0^*\,/\,\psi_0]$. Last, we shall a priori exclude the possibility of stiffness recovery by assuming a vanishing extra entropy supply such that the extra entropy flux $\boldsymbol{S}$

$$\boldsymbol{S} = \boldsymbol{0} \qquad (16)$$

and the extra entropy source $\mathcal{S}_0$

$$\mathcal{S}_0 = 0 \qquad (17)$$

vanish identically.

Remark 2.2: Interpretation of the mass flux
In the case of chemically reacting concrete, the mass flux $\boldsymbol{R}$ can be related to the transport of solved cations and anions Ca^{2+}, OH^-, $Al(OH)_4^-$, SO_4^{2-}, SiO_4^-, see e.g. (Ulm and Coussy 1995; Ulm, Torrenti, and Adenot 1999), (Torrenti, Mainguy, Adenot, and Tognazzi 1998), (Carmeliet 1998) or (Kuhl 2003) for detailed studies of moisture transport in the context of calcium leaching.

Remark 2.3: Interpretation of the mass source
In the context of chemomechanical damage of cementitious materials, the dissolution of portlandite or ettringite and the progressive decalcification of calcium silicate hydrates

$$\begin{aligned}
Ca(OH)_2 &\rightarrow Ca^{2+} + 2\,OH^- \\
Ca_6Al_2O_6(SO_4)_3 \cdot 32H_2O &\rightarrow 6\,Ca^{2+} \\
&+ 2\,Al(OH)_4^- + 3\,SO_4^{2-} \\
&+ 4\,OH^- + 26\,H_2O \\
Ca0 \cdot SiO_2 \cdot H_2O &\rightarrow Ca^{2+} + H_3SiO_4^- + H_2O
\end{aligned}$$
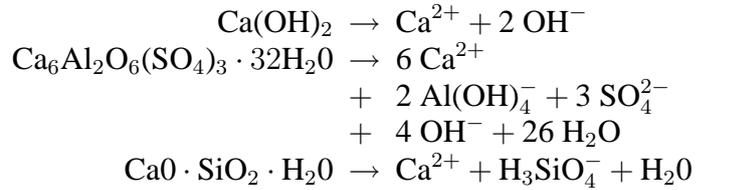
represent typical examples of changes in mass of the cementitious skeleton, see e.g. (Coussy 1995), (Kuhl and Meschke 2002) or (Stark and Wicht 2002) for detailed overviews. Recall, that in the absence of transport phenomena as $\boldsymbol{R} = \boldsymbol{0}$, the particular choice of $\mathcal{R}_0$ of equation (15) can be interpreted as an exponential damage evolution law

$$\mathrm{D}_t\, d = \exp[-\alpha\,\psi_0^*\,/\,\psi_0]$$

which characterizes an exponential increase of damage with increasing time and deformation.

2.4 *Weak form of the coupled problem*

While for classical chemomechanical applications, e.g. the leaching of portlandite, the capillary pressure and the deformation furnish the primary unknowns, we will introduce the reference density ρ_0 and the spatial deformation φ as primary unknowns within the mechanics of open systems. They are governed by the scalar–valued balance of mass (3) and by the vector–valued mass–specific balance of momentum (4) which can be cast into the corresponding residual statements with the residuals r^ρ and $\mathbf{r}^\varphi$ defined in the following form.

$$
\begin{aligned}
\mathsf{r}^\rho\,(\rho_0,\varphi) &= \quad \mathrm{D}_t\,\rho_0 - \mathrm{Div}\,\boldsymbol{R}\; - \mathcal{R}_0 = 0 \quad \text{in } \mathcal{B}_0 \\
\mathbf{r}^\varphi\,(\rho_0,\varphi) &= \rho_0\,\mathrm{D}_t\,\boldsymbol{p}\; - \mathrm{Div}\,\bar{\boldsymbol{\Pi}}^t - \bar{\boldsymbol{b}}_0 = \mathbf{0} \quad \text{in } \mathcal{B}_0
\end{aligned}
\tag{18}
$$

Herein, the boundary $\partial\mathcal{B}_0$ of the material domain can be decomposed into disjoint parts $\partial\mathcal{B}_0^\rho$ and $\partial\mathcal{B}_0^r$ for the density problem and equivalently into $\partial\mathcal{B}_0^\varphi$ and $\partial\mathcal{B}_0^t$ for the deformation problem. While Dirichlet boundary conditions are prescribed on $\partial\mathcal{B}_0^\rho$ and $\partial\mathcal{B}_0^\varphi$,

$$
\begin{aligned}
\rho_0 - \rho_0^{presc} &= 0 \quad \text{on } \partial\mathcal{B}_0^\rho \\
\varphi - \varphi^{presc} &= \mathbf{0} \quad \text{on } \partial\mathcal{B}_0^\varphi
\end{aligned}
\tag{19}
$$

Neumann boundary conditions can be given for the mass flux and the tractions on $\partial\mathcal{B}_0^r$ and $\partial\mathcal{B}_0^t$,

$$
\begin{aligned}
\boldsymbol{R}\;\cdot\boldsymbol{N} - r &= 0 \quad \text{on } \partial\mathcal{B}_0^r \\
\bar{\boldsymbol{\Pi}}^t\cdot\boldsymbol{N} - \boldsymbol{t} &= \mathbf{0} \quad \text{on } \partial\mathcal{B}_0^t
\end{aligned}
\tag{20}
$$

with $\boldsymbol{N}$ denoting the outward normal to $\partial\mathcal{B}_0$. As a prerequisite for the finite element discretization, the coupled set of equations has to be reformulated in weak form. To this end, the residual statements of the balance of mass and momentum (18) and the corresponding Neumann boundary conditions (20) are tested by the scalar– and vector–valued test function $\delta\rho$ and $\delta\varphi$, respectively.

$$
\begin{aligned}
\mathsf{g}^\rho\,(\delta\rho;\rho_0,\varphi) &= 0 \quad \forall\ \delta\rho \\
\mathsf{g}^\varphi\,(\delta\varphi;\rho_0,\varphi) &= 0 \quad \forall\ \delta\varphi
\end{aligned}
\tag{21}
$$

Thereby, the weak forms g^ρ and g^φ expand into the following expressions.

$$
\begin{aligned}
\mathsf{g}^\rho &= \int_{\mathcal{B}_0} \delta\rho\;\; \mathrm{D}_t\,\rho_0\;\mathrm{d}V + \int_{\mathcal{B}_0} \nabla\delta\rho\;\cdot\boldsymbol{R}\,\mathrm{d}V \\
&\quad - \int_{\partial\mathcal{B}_0^r} \delta\rho \quad r \quad \mathrm{d}A - \int_{\mathcal{B}_0} \delta\rho\;\;\mathcal{R}_0\,\mathrm{d}V \\
\mathsf{g}^\varphi &= \int_{\mathcal{B}_0} \delta\varphi\cdot\rho_0\,\mathrm{D}_t\,\boldsymbol{p}\,\mathrm{d}V + \int_{\mathcal{B}_0} \nabla\delta\varphi:\bar{\boldsymbol{\Pi}}^t\,\mathrm{d}V \\
&\quad - \int_{\partial\mathcal{B}_0^t} \delta\varphi\cdot\quad\boldsymbol{t}\quad\mathrm{d}A - \int_{\mathcal{B}_0} \delta\varphi\cdot\quad\bar{\boldsymbol{b}}_0\,\mathrm{d}V
\end{aligned}
\tag{22}
$$

3 DISCRETE EQUATIONS

3.1 *Temporal discretization*

For the temporal discretization of the governing equations (21), we partition the time interval of interest $\mathcal{T}$ into n_{step} subintervals $[t_n,t_{n+1}]$ as $\mathcal{T} = \bigcup_{n=0}^{n_{step}-1}[t_n,t_{n+1}]$ and focus on a typical time slab $[t_n,t_{n+1}]$ for which $\Delta t := t_{n+1} - t_n > 0$ denotes the actual time increment. Assume, that the primary unknowns ρ_{0n} and φ_n and all derivable quantities are known at the beginning of the actual subinterval t_n. In the spirit of implicit time marching schemes, we now reformulate the set of governing equations in terms of the unknowns ρ_{0n+1} and φ_{n+1}.

$$
\begin{aligned}
\mathsf{g}_{n+1}^\rho\,(\delta\rho;\rho_{0n+1},\varphi_{n+1}) &= 0 \quad \forall\,\delta\rho \\
\mathsf{g}_{n+1}^\varphi\,(\delta\varphi;\rho_{0n+1},\varphi_{n+1}) &= 0 \quad \forall\,\delta\varphi
\end{aligned}
\tag{23}
$$

Without loss of generality, we shall apply the classical Euler backward time integration scheme. Consequently, the first order material time derivatives $\mathrm{D}_t\rho_0$ and $\mathrm{D}_t\boldsymbol{p}$ can be approximated in the following form.

$$
\begin{aligned}
\mathrm{D}_t\,\rho_0 &= [\,\rho_{0n+1} - \rho_{0n}\,]\,/\,\Delta t \\
\mathrm{D}_t\,\boldsymbol{p} &= [\,\boldsymbol{p}_{n+1}\; - \boldsymbol{p}_n\;]\,/\,\Delta t
\end{aligned}
\tag{24}
$$

3.2 *Spatial discretization*

In the spirit of the finite element method, the domain of interest $\mathcal{B}_0$ is discretized into n_{el} elements $\mathcal{B}_0^e$ as $\mathcal{B}_0 = \bigcup_{e=1}^{n_{el}}\mathcal{B}_0^e$. The test functions $\delta\rho^h$ and $\delta\varphi^h$ and the trial function ρ^h and φ^h are interpolated on the element level with the basis functions N_ρ and N_φ, respectively.

$$
\begin{aligned}
\delta\rho^h &= \sum_{i=1}^{n_{e\rho}} N_\rho^i\,\delta\rho_i \qquad \delta\varphi^h = \sum_{j=1}^{n_{e\varphi}} N_\varphi^j\,\delta\varphi_j \\
\rho_0^h &= \sum_{k=1}^{n_{e\rho}} N_\rho^k\,\rho_k \qquad \varphi^h = \sum_{l=1}^{n_{e\varphi}} N_\varphi^l\,\varphi_l
\end{aligned}
\tag{25}
$$

Recall that the element set of density nodes $i = 1,\ldots,n_{e\rho}$ and the element set of deformation nodes $j = 1,\ldots,n_{e\varphi}$ can generally be chosen independently. With the above discretizations, the discrete residuals can be rewritten as follows.

$$
\begin{aligned}
\mathsf{r}_I^\rho &= \mathbf{A}_{e=1}^{n_{el}} \int_{\mathcal{B}_0^e} N_\rho^i\,\frac{\rho_{0n+1} - \rho_{0n}}{\Delta t} + \nabla N_\rho^i\cdot\boldsymbol{R}_{n+1}\;\mathrm{d}V \\
&\quad - \int_{\partial\mathcal{B}_0^{er}} N_\rho^i\quad r_{n+1}\,\mathrm{d}A \;\;- \int_{\mathcal{B}_0^e} N_\rho^i\mathcal{R}_{0n+1}\mathrm{d}V = 0 \\
\mathbf{r}_J^\varphi &= \mathbf{A}_{e=1}^{n_{el}} \int_{\mathcal{B}_0^e} N_\varphi^j\rho_0\,\frac{\boldsymbol{p}_{n+1} - \boldsymbol{p}_n}{\Delta t} + \nabla N_\varphi^j\cdot\bar{\boldsymbol{\Pi}}_{n+1}\;\mathrm{d}V \\
&\quad - \int_{\partial\mathcal{B}_0^{te}} N_\varphi^j\quad\boldsymbol{t}_{n+1}\,\mathrm{d}A \;\;- \int_{\mathcal{B}_0^e} N_\varphi^j\bar{\boldsymbol{b}}_{0n+1}\,\mathrm{d}V = \mathbf{0}
\end{aligned}
\tag{26}
$$

Herein, the operator $\mathbf{A}$ symbolizes the assembly of all element contributions at the element density nodes

$i = 1, \ldots, n_{e\rho}$ and the element deformation nodes $j = 1, \ldots, n_{e\varphi}$ to the overall residuals at the global density and deformation node points $I = 1, \ldots, n_{n\rho}$ and $J = 1, \ldots, n_{n\varphi}$.

4 LINEARIZED EQUATIONS

The discrete residual statements characterizing the mechanics of open systems (26) represent a highly nonlinear coupled system of equations which can be solved efficiently within the framework of a monolithic incremental iterative Newton–Raphson solution strategy. To this end, we perform a consistent linearization of the governing equations at time t_{n+1}

$$
\begin{aligned}
\mathsf{r}^{\rho \ k+1}_{I \ n+1} &= \mathsf{r}^{\rho \ k}_{I \ n+1} + \mathsf{d} \, \mathsf{r}^{\rho}_{I} \doteq 0 \quad \forall \, I = 1, \ldots, n_{np} \\
\mathbf{r}^{\varphi \ k+1}_{J \ n+1} &= \mathbf{r}^{\varphi \ k}_{J \ n+1} + \mathsf{d} \, \mathbf{r}^{\varphi}_{J} \doteq \mathbf{0} \quad \forall \, J = 1, \ldots, n_{np}
\end{aligned}
\tag{27}
$$

whereby the iterative residua dr^{ρ}_{I} and $\mathsf{d}\, \mathbf{r}^{\varphi}_{J}$ take the following format.

$$
\begin{aligned}
\mathsf{dr}^{\rho}_{I} &= \sum_{K=1}^{n_{n\rho}} \mathsf{K}^{\rho\rho}_{IK} \, \mathsf{d}\rho_K + \sum_{L=1}^{n_{n\varphi}} \mathbf{K}^{\rho\varphi}_{IL} \cdot \mathsf{d}\boldsymbol{\varphi}_L \\
\mathsf{d}\mathbf{r}^{\varphi}_{J} &= \sum_{K=1}^{n_{n\rho}} \mathbf{K}^{\varphi\rho}_{JK} \, \mathsf{d}\rho_K + \sum_{L=1}^{n_{n\varphi}} \mathbf{K}^{\varphi\varphi}_{JL} \cdot \mathsf{d}\boldsymbol{\varphi}_L
\end{aligned}
\tag{28}
$$

In the above definitions, we have introduced the following iteration matrices.

$$
\begin{aligned}
\mathsf{K}^{\rho\rho}_{IK} &= \mathop{\mathbf{A}}_{e=1}^{n_{el}} \int_{\mathcal{B}_0^e} N_\rho^i \ \frac{1}{\Delta t} \ N_\rho^k \, \mathrm{d}V \\
&\quad - \int_{\mathcal{B}_0^e} N_\rho^i \ \partial_{\rho_0}\mathcal{R}_0 \ N_\rho^k \, \mathrm{d}V \\
&\quad + \int_{\mathcal{B}_0^e} \nabla N_\rho^i \ \cdot R_0 \ \nabla N_\rho^k \, \mathrm{d}V \\
\mathbf{K}^{\rho\varphi}_{IL} &= \mathop{\mathbf{A}}_{e=1}^{n_{el}} - \int_{\mathcal{B}_0^e} N_\rho^i \ \partial_{\boldsymbol{F}}\mathcal{R}_0 \cdot \ \nabla N_\varphi^l \, \mathrm{d}V \\
\mathbf{K}^{\varphi\rho}_{JK} &= \mathop{\mathbf{A}}_{e=1}^{n_{el}} \int_{\mathcal{B}_0^e} \nabla N_\varphi^j \cdot \partial_{\rho_0} \bar{\boldsymbol{\Pi}}^t \ N_\rho^k \, \mathrm{d}V \\
\mathbf{K}^{\varphi\varphi}_{JL} &= \mathop{\mathbf{A}}_{e=1}^{n_{el}} \int_{\mathcal{B}_0^e} N_\varphi^j \rho_0 \frac{1}{\Delta t^2} \boldsymbol{I} \ N_\varphi^l \, \mathrm{d}V \\
&\quad + \int_{\mathcal{B}_0^e} \nabla N_\varphi^j \cdot \partial_{\boldsymbol{F}} \bar{\boldsymbol{\Pi}}^t \cdot \nabla N_\varphi^l \, \mathrm{d}V
\end{aligned}
\tag{29}
$$

The specification of the partial derivatives of the mass source $\mathcal{R}_0$, the mass source $\boldsymbol{R}$ and the reduced momentum flux $\bar{\boldsymbol{\Pi}}^t$ with respect to the primary unknowns ρ_0 and $\boldsymbol{\varphi}$ depends on the particular choice of the constitutive equations. For the constitutive equations suggested in section 2.3, we obtain the following

expressions,

$$
\begin{aligned}
\partial_{\rho_0} \ \mathcal{R}_0 &= \frac{1}{[1-d]} \frac{\psi_0^*}{\psi_0} \alpha \, \mathcal{R}_0 \\
\partial_{\boldsymbol{F}} \ \mathcal{R}_0 &= \frac{1}{\psi_0} \frac{\psi_0^*}{\psi_0} \alpha \, \mathcal{R}_0 \, \bar{\boldsymbol{\Pi}}^t \\
\partial_{\nabla\rho_0}\boldsymbol{R} &= R_0 \, \boldsymbol{I} \\
\partial_{\rho_0} \ \bar{\boldsymbol{\Pi}}^t &= \frac{1}{[1-d]} \frac{1}{\rho_0^*} \bar{\boldsymbol{\Pi}}^t \\
\partial_{\boldsymbol{F}} \ \bar{\boldsymbol{\Pi}}^t &= [1-d][\mu_0 \boldsymbol{I} \overline{\otimes} \boldsymbol{I} + \lambda_0 \boldsymbol{F}^{-t} \otimes \boldsymbol{F}^{-t} \\
&\quad -[\lambda_0 \ln(J) - \mu_0] \boldsymbol{F}^{-t} \underline{\otimes} \boldsymbol{F}^{-1}]
\end{aligned}
\tag{30}
$$

whereby the component representations of the non–standard dyadic products read $\{\bullet \overline{\otimes} \circ\}_{ijkl} = \{\bullet\}_{ik} \otimes \{\circ\}_{jl}$ and $\{\bullet \underline{\otimes} \circ\}_{ijkl} = \{\bullet\}_{il} \otimes \{\circ\}_{jk}$. Finally, the solution of the system of equations (27) renders the iterative update for the increments of the global unknowns ρ_I and $\boldsymbol{\varphi}_J$.

$$
\begin{aligned}
\Delta \ \rho_I &= \Delta \ \rho_I + \mathsf{d} \ \rho_I \quad \forall \, I = 1, \ldots, n_{n\rho} \\
\Delta \ \boldsymbol{\varphi}_J &= \Delta \ \boldsymbol{\varphi}_J + \mathsf{d}\boldsymbol{\varphi}_J \quad \forall \, J = 1, \ldots, n_{n\varphi}
\end{aligned}
\tag{31}
$$

5 EXAMPLES

Finally, we shall elaborate the proposed model in terms of a one–dimensional and two three–dimensional model problems.

5.1 *One–dimensional model problem*

To illustrate the physical nature of the constitutive introduced in section 2.3, figures 1 and 2 show the material response in a one–dimensional tension test. For the sake of transparency, we have neglected transport effects as $\boldsymbol{R} = \boldsymbol{0}$ such that the density evolution is governed by the mass source $\mathcal{R}_0$ alone. The reference density and the reference free energy are chosen to $\rho_0^* = 1.0$ and $\psi_0^* = 0.1$ while the exponent α takes the value of $\alpha = 0.25$. The Lamé constants of the free energy function introduced in equation (10) are chosen to $\lambda = 0.5769$ and $\mu = 0.3846$. In particular, the curves in figure 1 show the evolution of damage versus the stretch λ for different time step sizes t. The value of the damage variable starts at zero and increases exponentially with increasing stretches until it finally converges to one. Thereby, the onset of damage is, of course, more pronounced for larger time scales. The curves in figure 2, on the contrary, depict the evolution of damage versus time for different stretches λ. For larger stretches, the evolution of damage obviously proceeds faster than for moderate stretches. In contrast to commonly applied time–independent damage models, the model suggested herein is not determined by the amount of loading alone. Rather, the specimen damages further upon constant loading
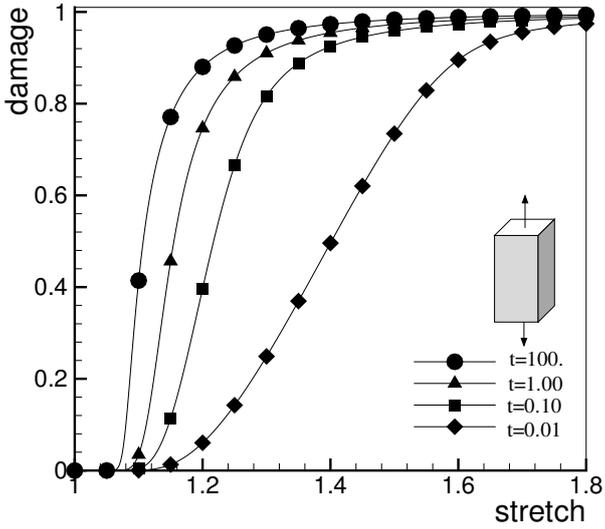
Figure 1: Evolution of damage with stretch

Figure 3: Tension problem – Displacement and force

Figure 2: Evolution of damage with time
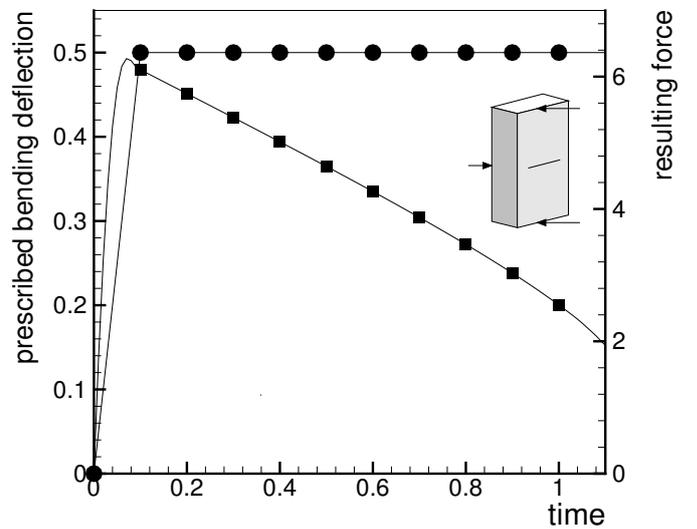
Figure 4: Bending problem – Displacement and force

as time evolves. From a physical point of view, this property of the model captures the effect of ageing in a natural and straightforward way. Moreover, from a continuum point of view, the inclusion of rate effects essentially stabilizes the formulation, in particular in the post–critical regime.

5.2 *Three–dimensional simulation*

Finally, we elaborate the three–dimensional response of the derived chemomechanical damage model in tension and bending. The specimen has a length : width : height ratio of 2 : 1 : 0.5 and is discretized with 24 : 12 : 6 trilinear Q1Q1 elements. The material parameters are chosen to $\lambda = 288.46$, $\mu = 192.31$, $\rho_0^* = 1.0$, $\psi_0^* = 1.0$ and $\alpha = 2.5$, whereas the mass conduction coefficient is set equal to zero as $R_0 = 0$.
Since we aim at predicting the post–peak response of the specimen, the load is applied by displacement control. Figures 3 and 4 shows the prescribed top and bottom displacement and the prescribed bending deflection which both are increased during the first

ten time steps of $\Delta t = 0.01$ and then held constant for another 90 time steps. Both figures nicely reflect the fact that the overall load carrying capacity drops down considerably at the onset of damage. For both, the tension and the bending problem, the resulting spatial force reduces to about a third of its maximum value due to the damage induced stiffness degradation.
Figures 5 and 6 depict the corresponding evolutions of the density, the deformation and the discrete material surface forces for the tension, the bending and the torsion problem. Thereby, the five different stages depicted in the figures correspond to time step 2 right at the beginning of the loading phase, to time step 10 at the end of the load increase and to time step 40, time step 60 and time step 100 which illustrate the onset of damage upon constant prescribed deformation. Mechanical loading obviously induces a reduction of the load carrying capacity accompanied by a localization of the deformation in narrow bands. As damage evolves, this localization becomes more

and more pronounced while the remaining parts of the structure tend to unload almost completely.

6 CONCLUSIONS

A general theoretical and computational framework for the thermodynamics of open systems has been presented which is particularly suited for chemomechanical applications. The formulation is based on the simultaneous solution of the balance of mass and momentum which essentially govern the evolution of the density and the deformation field. The particularly appealing feature of the proposed formulation is based on the fact that we no longer deal with an 'artificial' internal damage variable which we cannot determine explicitly in experiments but that we rather introduce damage as a change of the current reference density which can obviously be accessed directly through appropriate experimental setups. Numerical results have been derived and discussed for a one–dimensional model problem as well as for a three–dimensional tension and bending test. It should be pointed out, that in contrast to classical time–independent damage simulations, we did not encounter any algorithmic problems throughout all the analyses, even when we calculated far into the softening branch. The incorporation of time–dependent effects apparently regularizes the underlying damage formulation. Stability might also have been enhanced due to the fact that damage was interpolated continuously on the node point level in contrast to most classical damage formulations which typically suggest an integration point based approach.

REFERENCES

Bowen, R. M. (1976). Theory of mixtures. In A. C. Eringen (Ed.), *Continuum Physics – Volume III – Mixtures and EM Field Theories*, pp. 1–127. Academic Press, New York – San Francisco – London.

Carmeliet, J. (1998). A poroviscoelastic damage model for hygromechanical damage processes in unsaturated porous media. In R. de Borst, N. Bićanić, H. Mang, and G. Meschke (Eds.), *Computational Modelling of Concrete Structures*, pp. 559–566. Balkema, Rotterdam.

Coussy, O. (1995). *Mechanics of Porous Continua*. John Wiley & Sons.

de Boer, R. (2000). *Theory of Porous Media – Highlights in the Historical Development and Current State*. Springer Verlag, Berlin – Heidelberg – New York.

Epstein, M. and G. A. Maugin (2000). Thermomechanics of volumetric growth in uniform bodies. *Int. J. Plasticity 16*, 951–978.

Katchalsky, A. and P. F. Curran (1965). *Nonequilibrium Thermodynamics in Biophysics*. Harvard University Press – Cambridge, Massachusetts.

Kuhl, D. (2003). Ion diffusion models based on the Debye–Hückel–Onsager theory applied to calcium leaching of cementitious materials. *J. Struct. Eng., ASCE, submitted for publication*.

Kuhl, D. and G. Meschke (2002). Higher order transport models for the simulation of dissociation–diffusion processes in reactive porous media. In H. A. Mang, F. G. Rammerstorfer, and J. Eberhardsteiner (Eds.), *WCCM V, Fifth World Congress on Compuational Mechanics*.

Kuhl, E. and P. Steinmann (2003a). Computational modeling of healing: An application of the material force method. *Biomechanics and Modeling in Mechanobiology, accepted for publication*.

Kuhl, E. and P. Steinmann (2003b). Mass– and volume specific views on thermodynamics for open systems. *Proceedings of the Royal Society of London 459*, 2547–2568.

Kuhl, E. and P. Steinmann (2003c). Material forces in open system mechanics. *Comp. Meth. Appl. Mech. Eng., accepted for publication*.

Kuhl, E. and P. Steinmann (2003d). On spatial and material settings of thermo–hyperelastodynamics for open systems. *Acta Mechanica 160*, 179–217.

Kuhl, E. and P. Steinmann (2003e). Theory and numerics of geometrically non–linear open system mechanics. *Int. J. Num. Meth. Eng. 58*, 1593–1615.

Stark, J. and B. Wicht (2002). *Dauerhaftigkeit von Beton – Der Baustoff als Werkstoff*. Birkhäuser, Basel – Boston – Berlin.

Torrenti, J.-M., M. Mainguy, F. Adenot, and C. Tognazzi (1998). Modelling of leaching in concrete. In R. de Borst, N. Bićanić, H. Mang, and G. Meschke (Eds.), *Computational Modelling of Concrete Structures*, pp. 531–538. Balkema, Rotterdam.

Truesdell, C. and R. Toupin (1960). The classical field theories. In S. Flügge (Ed.), *Handbuch der Physik*, Volume III/1. Springer Verlag, Berlin.

Ulm, F.-J. and O. Coussy (1995). Modelling of thermomechanical coupling of concrete at early ages. *J. Eng. Mech. 121*, 785–794.

Ulm, F.-J., J.-M. Torrenti, and F. Adenot (1999). Chemoporoplasticity of calcium leaching in concrete. *J. Eng. Mech. 125*, 1200–1211.
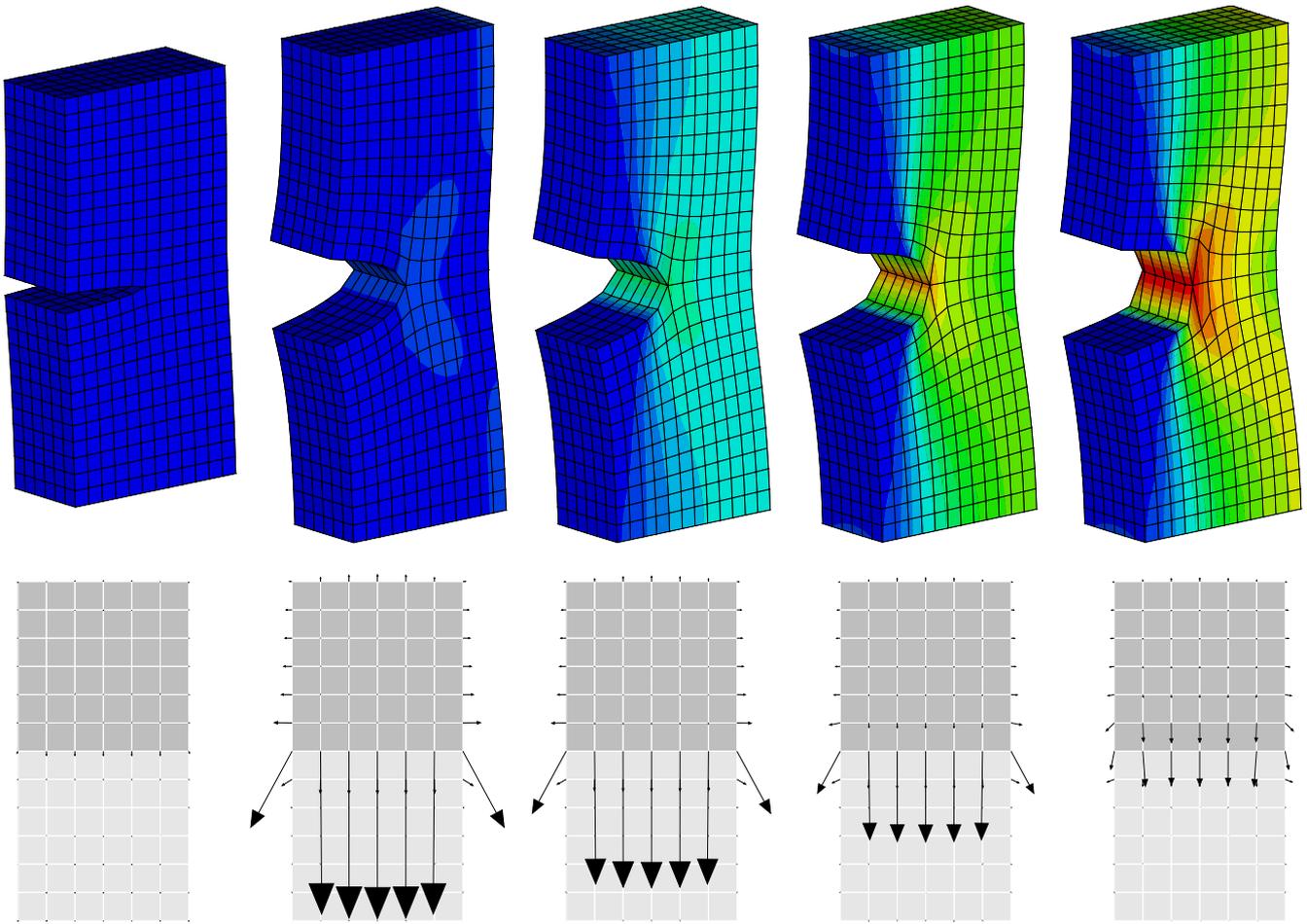
Figure 5: Tension problem – Evolution of density and material forces
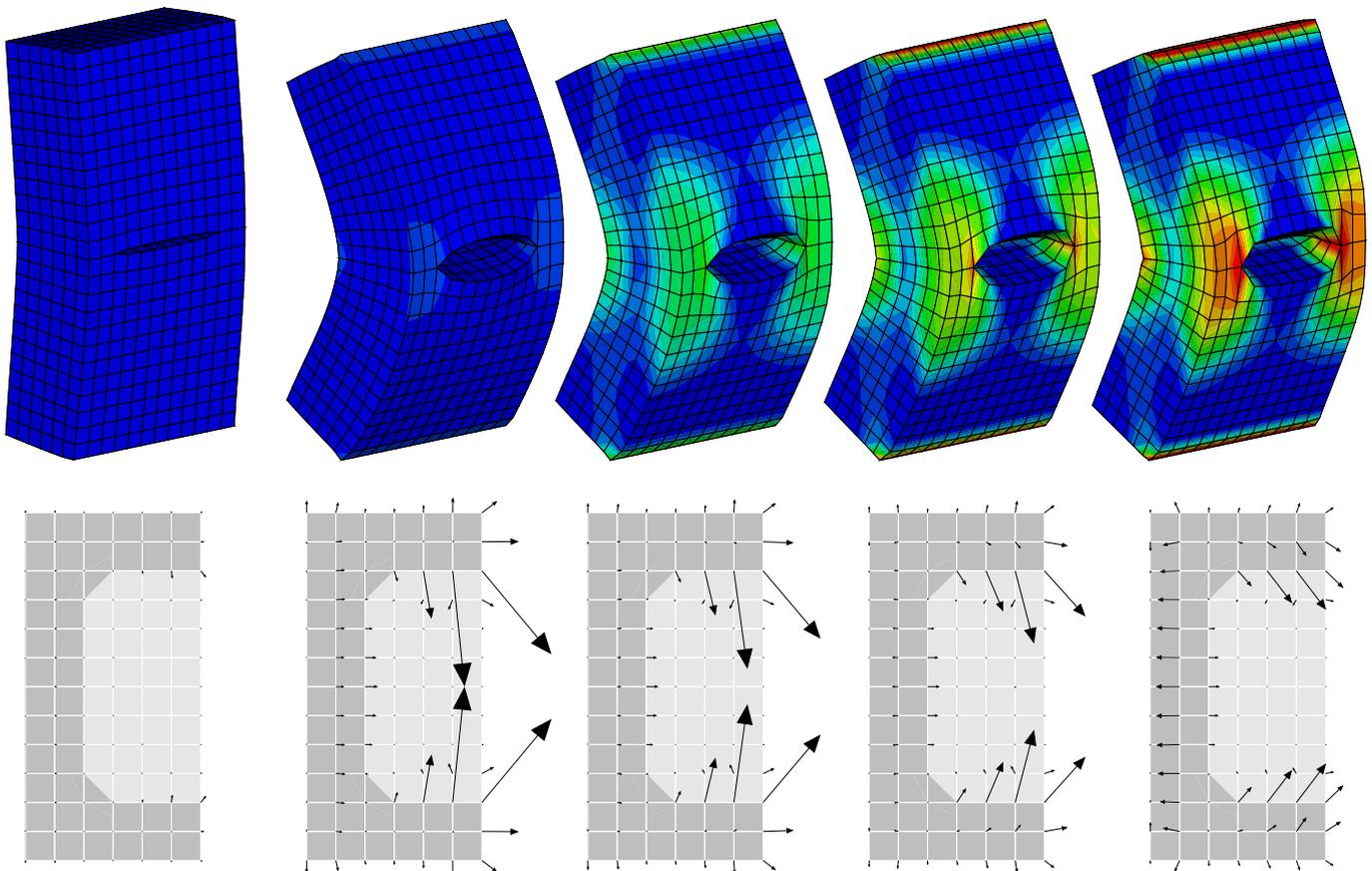
Figure 6: Bending problem – Evolution of density and material forces